DAMAGE ASSESSMENT USING ALOS-2/PALSAR-2 FOR THE 2018 EARTHQUAKE IN PALU, SULAWESI, INDONESIA

Nopphawan Tamkuan, Masahiko Nagai

Yamaguchi University, 2-16-1, Tokiwadai, Ube, Yamaguchi, 755-8611, Japan
Email: nopphawan.yui@gmail.com, nagaim@yamaguchi-u.ac.jp

KEY WORDS: ALOS-2/PALSAR-2, Damage Assessment, Interferometric Coherence

ABSTRACT: On 28 September 2018, 7.5 magnitude earthquake occurred in the island of Sulawesi, Indonesia. The earthquake triggered a tsunami in the coastal zone and induced severe liquefaction. This earthquake led to high number of losses, injuries and damaged houses. Rapid damage assessment can support and reduce impacts after the unpredictable earthquake. ALOS-2/PALSAR-2, a synthetic aperture radar (SAR) plays an important role in disaster management. It can observe night and daytime with less interference of atmospheric conditions and high frequency of observation. This study analyzed two observation modes of ALOS-2 including ScanSAR (WD1) and Stripmap (SM3). These two modes consist of horizontal transmit-horizontal receive (HH) and horizontal transmit-vertical receive (HV) polarizations. Two archived images before earthquake and one image after the earthquake of each mode and polarization were analyzed for interferometric coherence. The change of coherence pairs (before- and between-events) was implemented to estimate damage and effected areas. The ALOS-2 products were evaluated for capacity assessment by comparing more than 10,000 locations of ground truth. High coherence change was strongly related to damaged areas. The result found that Stripmap mode provided higher accuracy compare to ScanSAR and HH indicated more potential to detect damage area in the central of Sulawesi. Moreover, the analyzed results were compared to Sentinel-2 image and SAR intensity change that presented completely damaged areas. The comparison showed good agreement in complete damage or destroyed area. Moreover, damage mapping by this technique can reveal less to moderate damage which cannot be presented by those optical image and SAR intensity methods. It can be implemented to monitor recovery process and support disaster management.

1. INTRODUCTION

The massive earthquake (7.5 magnitude) hit Sulawesi island on 28 September 2018. The epicenter was located 77 km. away from Palu city. This event affects central of Sulawesi and very high impact on Palu city, Donggala, Sigi and Parigi Moutong. This earthquake induced major soil liquefaction and tsunami in the long coastal zone. It caused more than 2000 fatalities, 68,000 damaged houses, and more than 200,000 internally displaced persons (AHA Centre, 2018). Earthquake brings highest number of human deaths compare other disaster. Moreover, it is sudden and devastate event and difficult to predict. Rapid response should be applied after disaster to minimize the effect from earthquake.

SAR plays very important role in emergency observation for disaster. In emergency, satellite images must be rapidly analysed as soon as possible after data acquisition. The earthquake in Sulawesi was selected to be study area due to severity of this event. The emergency observation had been activated by many organizations or initiatives as such Sentinel-Asia and Disaster Charter. ALOS-2 is one of the effective emergency satellite observations and it has provided many SAR images for many disasters in Asia and in the case of earthquake in Sulawesi in 2018. Disaster is unpredictable event. Training data and validation is difficult to collect and conduct just after the disaster (in early response phase). Therefore, previous disasters should be analysed more to learn for preparing and awareness for unpredictable disaster.

Interferometry technique have been applied for earthquake deformation in Palu, Indonesia (Fang et al., 2019) and crustal deformation in Nepal (Kobayashi, Morishita, & Yarai, 2015) and other disaster related surface movement. Moreover, interferometric coherence has been implemented to damage assessment without training data for this decade (Plank, 2014). The common method needs two SAR image before earthquake and one image after earthquake. The change of interferometric coherence could present well for damage building. For example, ALOS-2 showed high accuracy of damage assessment for the 2016 Kumamoto earthquake in Japan (Tamkuan & Nagai, 2017). Likewise, other sensor Sentinel-1 could detect damage area by the similar method (Tamkuan & Nagai, 2019). Moreover, soil liquefaction areas from Tohoku earthquake in 2011 could be detected using ALOS-1 (Ishitsuka, Tsuji, & Matsuoka, 2013). ALOS-2 has potential to detect individual building. Interferometric analysis of ALOS-2 (SM1 mode) was assessed for sensitivity and limitation for assessing individual damaged building (Natsuaki, Nagai, Tomii, & Tadono,

2018). ALOS-2 has many types of observation modes. In case of dual-polarizations or more, it is questionable to select which data should be analyzed first. Furthermore, the assessment between different modes and polarization has not or less conducted.

Accordingly, the objective of this research is to evaluate ALOS-2 products by different mode (ScanSAR and Stripmap) and different polarization (HH and HV) for detecting damaged areas induced by earthquake. The benefits of this study are to learn capacity of each mode and their polarization. The validation of data will be a benefit for deciding priority to process first in case of emergency. Moreover, it is to realize and extract necessary information for supporting decision making not only for quick response but also to implement in recovery phase and other disaster management.

2. DATA AND SOFTWARE USED

Two different observation mode were operated in this study including Stripmap mode (or SM3 operation mode) and ScanSAR mode (or WD1 operation mode). All images were obtained with level 1.1 or Single Look Complex (SLC) products. Digital elevation model (DEM) from ASTER GDEM had been used for interferometry processing. These two modes of observation provide dual polarizations including HH and HV. Stripmap mode has higher spatial resolution. ScanSAR has lower spatial resolution but it covers very large area. In this study, just sub-swath F1 could cover the earthquake effected areas. Two images before and one image after the earthquake were analysed for the change of interferometric coherence of earthquake damaged areas. Information of used images are shown in Table 1. This study was analysed using only open source and free software. GMTSAR (Sandwell et al., 2016) has been used for interferometry processing and QGIS for other processing.

Table 1. ALOS-2 images used in this study

ALOS-2 images	Acquisition date	Mode	Look direction	Flight direction	Earthquake
ALOS2222973600-180710	10-Jul-2018	WD1	Right	Descending	Before
ALOS2229183600-180821	21-Aug-2018	WD1	Right	Descending	Before
ALOS2235393600-181002	2-Oct-2018	WD1	Right	Descending	After
ALOS2214177170-180511	11-May-18	SM3	Right	Ascending	Before
ALOS2228667170-180817	17-Aug-18	SM3	Right	Ascending	Before
ALOS2236947170-181012	18-Oct-2018	SM3	Right	Ascending	After

3. METHODOLOGY

3.1 Interferometry Technique

Interferometry technique is the geodetic technique to identify ground movement and deformation of the earth using repeat-pass interferometry (Hanssen, 2002). This technique is very useful for disasters related to ground deformation. It can provide quickly observed earthquake deformation in all kind of weathers and large coverage at centimetre-level accuracy for measuring surface displacement of such as crustal movement by the earthquake, glacier flow measurement, surface deformation by volcanic activity, landslides and land subsidence. Interferometric analysis was used to detect earthquake rupture and damage potential area by the change of interferometric coherence. This analysis was processed by GMTSAR. DEM was used in the processing for detecting deformation and geo-coding the images.

3.2 Interferometric Coherence

Correlation or coherence is one of the interferometric products. It has the advantages to determine the quality of the interferometric measurement (interferogram) and extract thematic information about the object on the ground. It describes SAR backscattering characteristics changed by the ground surface changes and collapse or damage of the buildings (Yonezawa & Takeuch, 1995). The coherence (Υ) is defined as the magnitude of the cross-correlation coefficient between two co-registered complex images as described by the equation 1:

$$\Upsilon = \frac{|\langle S_1 S_2^* \rangle|}{\sqrt{\langle S_1 S_1^* \rangle \langle S_2 S_2^* \rangle}} \quad (1)$$

Where S1 and S1 are the corresponding complexes of two single look complex. S* is complex conjugate of S. It ranges from 0 (no correlation) to 1 (perfect correlation).

There are many sources of decorrelations resulting from the analysis. Such decorrelation includes other effects that could be considered (Ishitsuka et al., 2013). Coherence comprises of contributions from three main effects (Zebker & Villasenor, 1992) as shown in equation 2.

$$\Upsilon = \Upsilon_{noise}\,\Upsilon_{geom}\,\Upsilon_{temp} \quad (2)$$

where Υ_{noise} represents noise in the radar system and processing approach, Υ_{geom} is geometric coherence proportional to the perpendicular component of the baseline, and Υ_{temp} is the influence of temporal backscatter change, e.g. from surface cover change or vegetation.

3.3 Interferometric Coherence Change

For quick response, interferometric coherence is useful and timely to support disaster management. The interferometric coherence of pre- and co-event can be utilized for damage assessment (Plank, 2014; Arciniegas, Bijker, Kerle, & Tolpekin, 2007). This study applies simple difference (Υ_{diff}) (equation 3) to investigate damage areas (Stramondo, Bignami, Chini, Pierdicca, & Tertulliani, 2006) with Υ_{pre} representing the pre-earthquake SAR image pair and Υ_{co} representing a pre- and a co-earthquake image pair.

$$\Upsilon_{diff} = \Upsilon_{pre} - \Upsilon_{co} \quad (3)$$

The high-level index presents high level of surface physical changes due to damaged area. The change of interferometric coherence is timely analysis in a wide area for rapid damage assessment.

3.5 Ground truth for the assessment

Ground truth information is necessary to be used for ALOS-2 capacity assessment as shown in Figure 1. There are many sources to investigate and compare with ALOS-2 products as shown in Table 2. Copernicus is one of the excellent sources which provides damage assessment immediately after the earthquake by interpreting very high-resolution images (Copernicus, 2018). The information was selected from specific extent between latitude -0.8 to -1.02 degree and longitude 119.80 to 119.96 degree. Moreover, some other information was interpreted and collected by using google earth image (imagery date on 2 October 2018). However, non-damaged buildings are probably including structural and non-structural damage, but it could not check damage from google earth image.

Table 2. Ground truth for the assessment

Group	Information	Number of locations	Sources
A	Non-damage	407	Google earth image
B	Assigned damage	324	Google earth image
C	Damage	5123	Copernicus
D	Destroy	5352	Copernicus

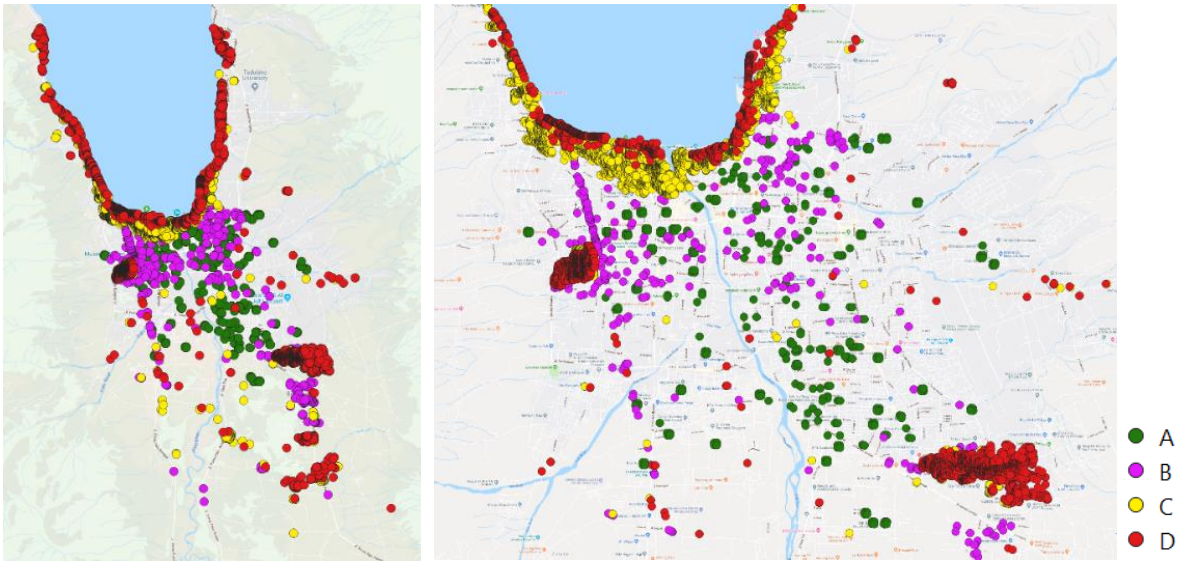

Figure 1. Ground truth for the assessment

3.4 ALOS-2 products capacity assessment

ScanSAR (WD1) and Stripmap (SM3) modes of ALOS-2 provide dual-polarizations (HH and HV). The ALOS-2 products capacity assessment was evaluated by interferometric coherence change as show in Figure 2. Also, each polarization was compared with ground truth from Copernicus and the assigned information from google earth image.

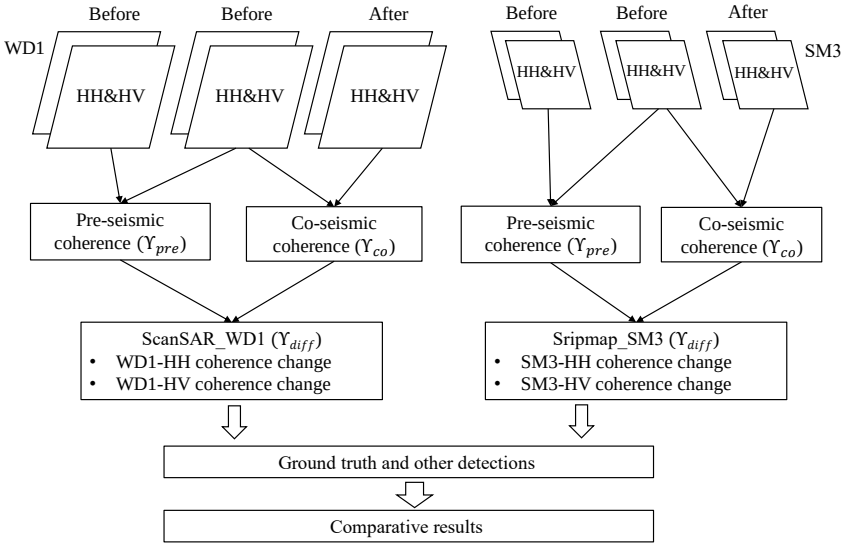

Figure 2. Overall framework for ALOS-2 products capacity assessment

4. RESULTS

4.1 Interferometric Coherence

Spatial resolution was default from the processing. ScanSAR (WD1) and Stripmap (SM3) coherence images were generated to be 90 m and 45 m respectively. For interferometric analysis, temporal baseline and perpendicular baseline are the key factors to evaluate the quality of interferometric products. From interferometric pairs, the absolute temporal baselines (Table 3) were not more than 360 m. (lower than critical baseline) that they are acceptable products and can be used for damage assessment. Theoretically, urban area provides strong coherence than other landcover types (such as vegetated area and waterbody). Coherence was presented higher value for normal situation and lower value in earthquake situation. From Table 4, HH polarization provided higher coherence compare to HV polarization. The coherence was decorrelated because surface movement and damage of building was quite clearly demonstrated by the Figure 3.

Table 3. Information of temporal, perpendicular and parallel baseline for interferometry analysis

InSAR Pair	Pair dates	Temporal baseline	Perpendicular baseline	Parallel baseline
Pair 1_WD1	180710-180821	42 days	-358.45 m.	-179 m.
Pair 2_WD1	180821-181002	42 days	50.36 m.	34.57 m.
Pair 1_SM3	180511-180817	98 days	28.98 m.	4.55 m.
Pair 2_SM3	180817-181012	62 days	332.05 m.	161.31 m.

Table 4. Statistical information of pre-seismic and co-seismic coherence for each damage groups

Modes	Information	Pre-seismic coherence				Co-seismic coherence			
		HH		HV		HH		HV	
		Mean	Std	Mean	Std	Mean	Std	Mean	Std
WD1	A: Non-damage	0.568	0.087	0.469	0.095	0.286	0.158	0.204	0.113
	B: Assigned damage	0.550	0.080	0.389	0.116	0.166	0.107	0.113	0.062
	C: Damage (Copernicus)	0.536	0.111	0.398	0.090	0.187	0.108	0.129	0.062
	D: Destroy (Copernicus)	0.498	0.137	0.394	0.127	0.138	0.121	0.111	0.071
SM3	A: Non-damage	0.722	0.120	0.544	0.134	0.409	0.171	0.323	0.158
	B: Assigned damage	0.614	0.147	0.431	0.162	0.164	0.129	0.134	0.105
	C: Damage (Copernicus)	0.643	0.134	0.490	0.144	0.267	0.143	0.219	0.127
	D: Destroy (Copernicus)	0.614	0.156	0.428	0.177	0.106	0.082	0.093	0.055

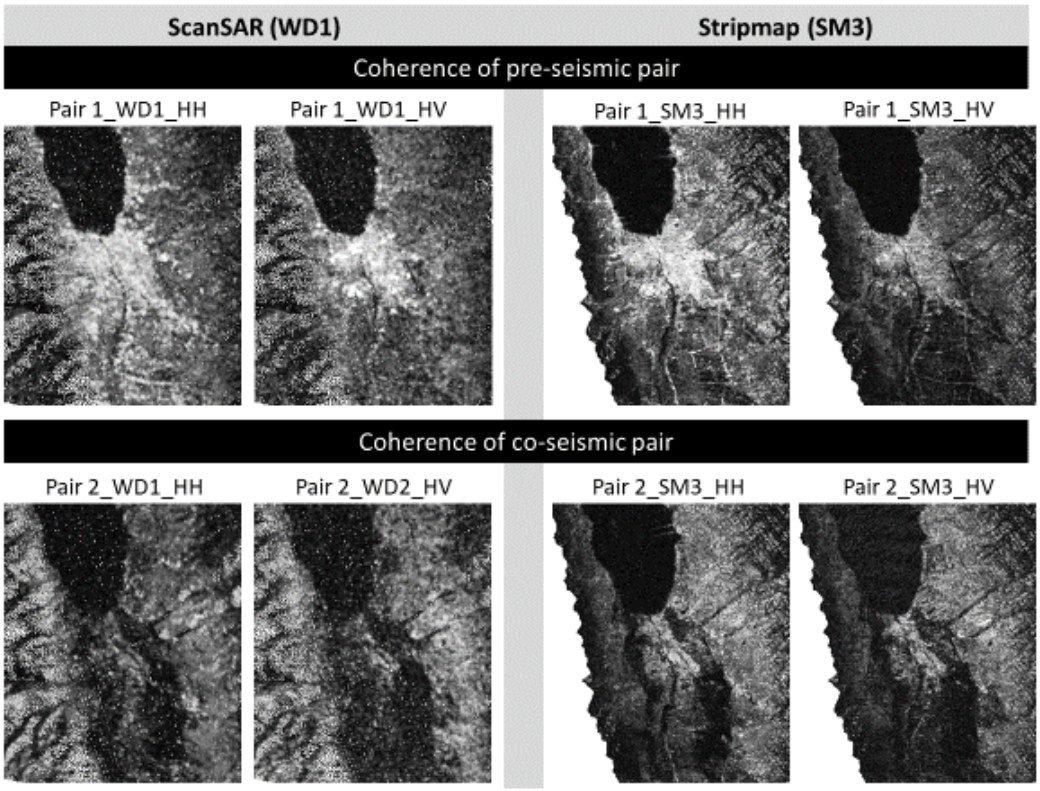

Figure 3. Interferometric coherence of HH and HV for co-seismic and pre-seismic pair (white is high value; black is low value)

4.2 Interferometric Coherence Change

The interferometric coherence change is the difference between pre-seismic and co-seismic pair. The degree of change is presented in Figure 4 by using boxplot format because of un-equality of ground truth. Figure 5 shows interferometric coherence change maps of each mode and polarization. ScanSAR (WD1) mode showed slight change between each damaged group. Stripmap (SM3) with higher spatial resolution showed moderate change of the ground truth distribution between classes. It showed the higher change between non-damage (A) and destroyed building (D) more than between non-damage (A) and damaged buildings (B). HH polarization provided more potential to differentiate between each group more than HV polarization. Table 5 presents the estimated overall accuracy of each mode and polarization. SM3-HH showed the highest accuracy for those observation modes and from different orbit and look direction.

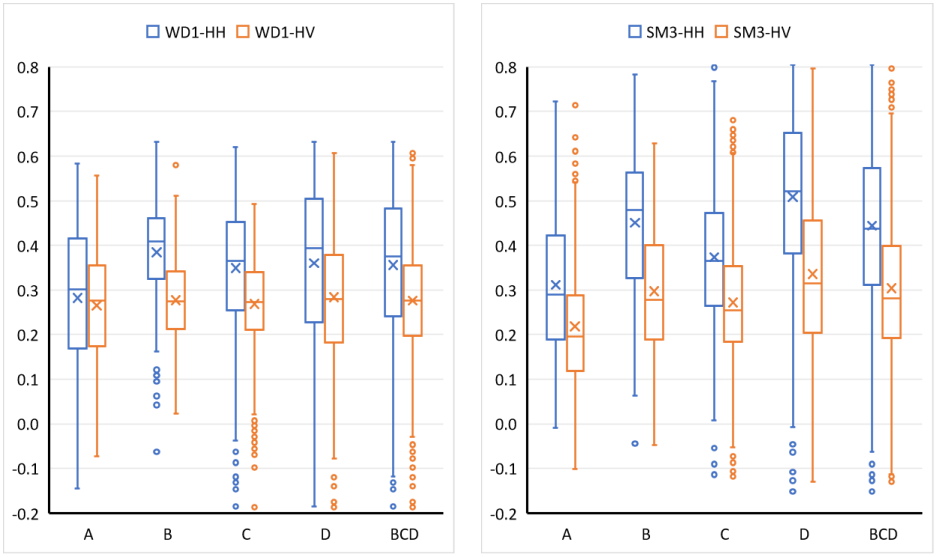

a) b)

Figure 4. Boxplot of each ground truth group and coherence change

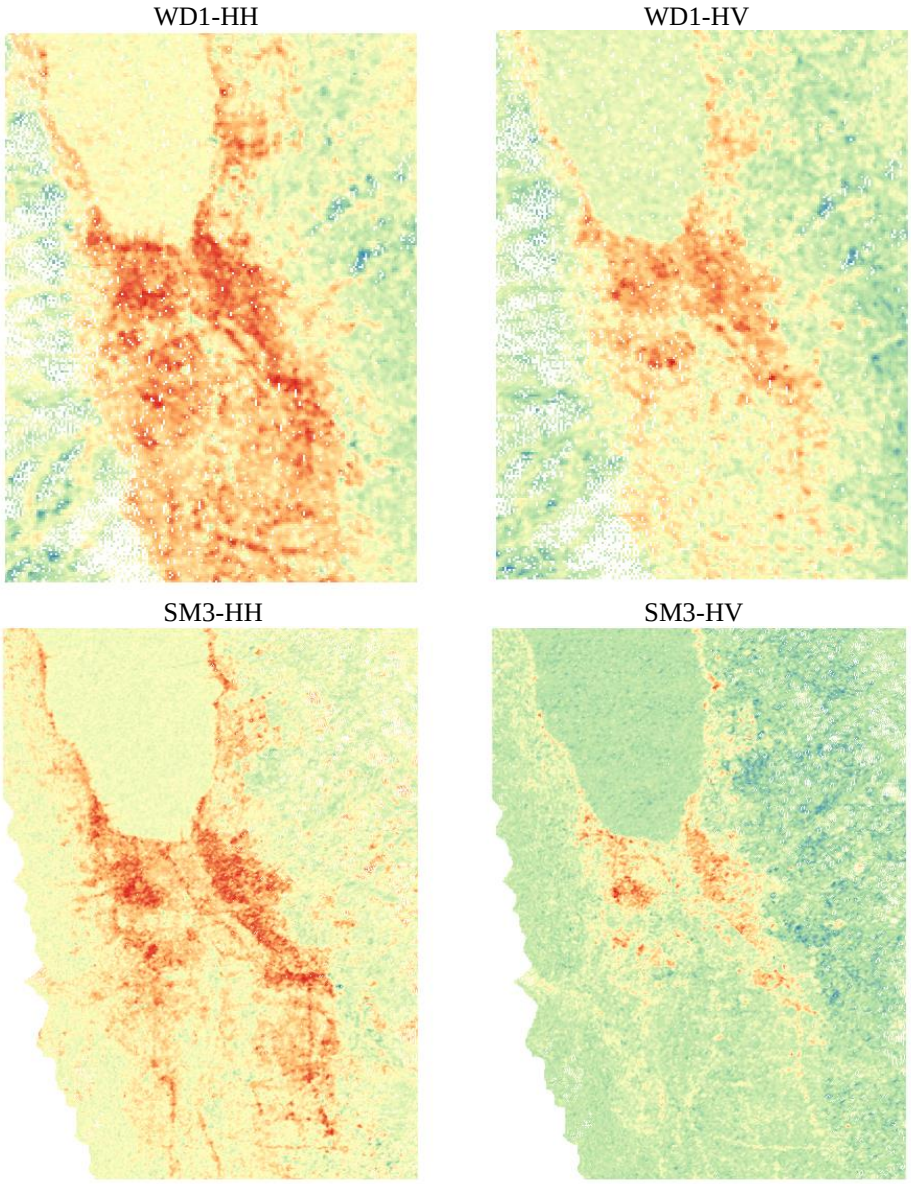

Figure 5. Interferometric coherence change maps (Red is high value; blue is low value)

Table 5. The estimated overall accuracy of each mode and polarization

Information	Threshold** median(A) - median (BCD)	Overall accuracy
WD1-HH	0.339	57.00%
WD1-HV	0.277	49.80%
SM3-HH	0.364	65.09%
SM3-HV	0.239	61.27%

** It is important to be note that threshold was evaluated by group A and BCD. Group A presents for non-damage area, but it might be the damaged buildings that could not be presented from google earth. Therefore, this assessment is for comparison purpose to different polarizations and modes only.

5. DISCUSSIONS

This study designed to evaluate ALOS-2 products capacity for earthquake assessment. Two observation modes were conducted including WD1 and SM3 modes. Moreover, different polarization (HH and HV) were compared and evaluated. This study considered just two images before earthquake and one image after earthquake for coherence change analysis. The result suggested HH is more appropriate to detect damage by interferometric coherence change more than HV data. Stripmap mode with HH polarization provided the best result in term of acquisition system and its spatial resolution for the 2018 earthquake in Indonesia.

For other change detections (Figure 6), they could represent only very high damage and complete destroy by liquefaction and tsunami. To compare optical satellite imagery (Figure 6-a), Sentinel-2 with 10 m. spatial resolution was analyzed by multivariate alteration detector algorithm (Nielsen & Conradsen, 1997) using image before (on 27 September 2018) and after-earthquake (on 2 October 2018). Moreover, ALOS-2 intensity change was analyzed to compare the result of this study by color-composite of HH polarization (Figure 6-b) and HV polarization (Figure 6-c) by using image on 18 October 2018 in red band, 17 August 2018 in green band and 11 May 2018 in blue band. From the results, interferometric coherence change could give more information which optical image could not present. Thus, result of damage area showed a wider range from minimal surface change to completely destroyed buildings. This method showed a potential to detect less damaged buildings more than using optical image and SAR intensity change.

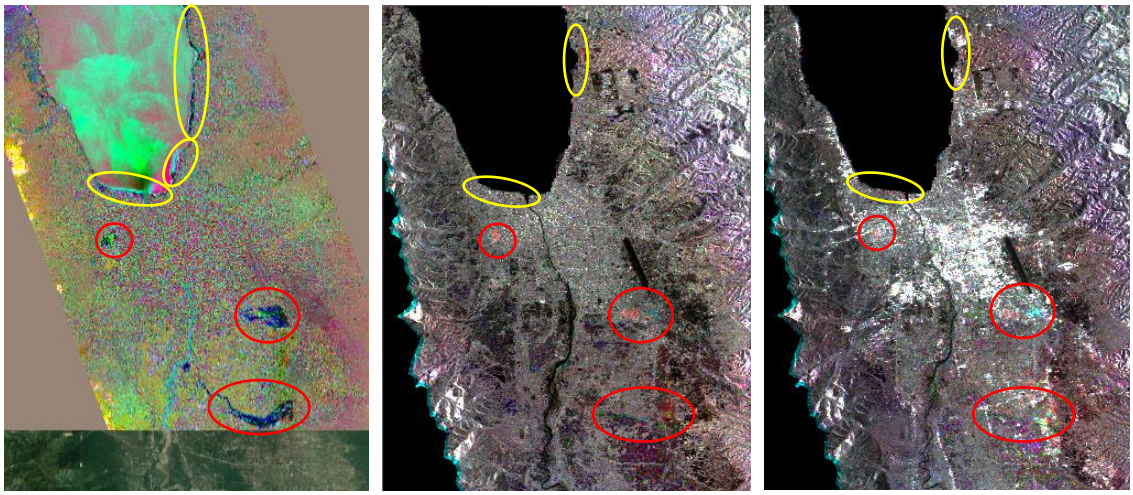

a b c

Figure 6. Other change detections (red highlights liquefaction, yellow highlights tsunami), a) Sentinel-2 color-composite of the change between before- and after-event images b) color-composite of HH polarization of ALOS-2 intensity backscatter c) color-composite of HV polarization

The ground truth is point locations based on Copernicus and google earth images. This information was assigned by high resolution image. In the real situation, some damage areas were not observable by high resolution image such as the damage because of little subsidence of building. Also, the top view of damaged buildings could present same as non-damage buildings. Ground truth in this study was categorized into 4 types: destroy (Copernicus), damage (Copernicus), assigned damage (google earth) and non-damage (google earth). There were unequal numbers of locations. Non-damaged locations were the location that probably non-damage decided by just google earth images. It probably includes structural and non-structural damages that could not assign from high resolution of optical images. However, this study could present more information about ALOS-2 capacity for damage assessment. It can comparatively summarized ALOS-2 products. HH coherence change was better applicable for Palu area more than HV in case of analysis in emergent case.

For future recommendations, this study evaluated only by points but result show as grid. Therefore, grid assessment with buildings density will be investigated for next study. More SAR images should be analyzed to minimize the other decorrelation effects that were not from ground movement related to damaged areas. For emergency mapping activity, consideration of using multi-sensor and multi-temporal images can rapidly provide more information. More advance techniques can be developed and applied for improving accuracy for monitoring damaged areas. Finally, this method can be used to support decision making in emergent situation and beneficial for further related applications such as recovery monitoring.

6. CONCLUSIONS

ALOS-2 satellite rapidly provided data to support the serious earthquake in Palu, Sulawei, Indonesia. The study presents the potential of different polarizations and observation modes including ScanSAR (WD1) and Stripmap (SM3). The interferometric coherence change using pre-seismic and co-seismic pairs were used to assess the capacity of ALOS-2 products for detecting building damage. There were more than 10,000 locations for ground truth for accuracy assessment. ScanSAR showed lower accuracy compare to Stripmap mode because of its spatial resolutions. The results of the coherence change can reveal less to moderate damage which cannot be presented by SAR intensity

and optical images. Comparative results between HH and HV polarization of these two modes, it was revealed that HH had more potential to detect damage area in the central of Sulawesi. However, this study suggests HH polarization of Stripmap mode to be implemented for more detail damage assessment. This study considered only the interferometric change method that used two images before and one image after earthquake and evaluated only by points-based assessment. Further research mentioned in future recommendation section are required. This research can be extended to cover other disaster management purposes.

ACKNOWLEDGEMENT

The authors gratefully acknowledge Japan Aerospace Exploration Agency (JAXA) for providing ALOS-2 data and Copernicus for providing building damage dataset.

REFERENCES

AHA Centre. (2018). *AHA-Centre-Annual-Report-2018-Singular*. Retrieved from https://ahacentre.org/wp-content/uploads/2019/07/AHA-CENTRE-ANNUAL-REPORT-2018-Singular.pdf

Arciniegas, G. A., Bijker, W., Kerle, N., & Tolpekin, V. A. (2007). Coherence- and amplitude-based analysis of seismogenic damage in Bam, Iran, using ENVISAT ASAR data. *IEEE Transactions on Geoscience and Remote Sensing*, *45*(6), 1571–1581. https://doi.org/10.1109/TGRS.2006.883149

Copernicus. (2018). Sulawesi Earthquake 2018, Copernicus Building Damage Classification. Retrieved March 1, 2019, from https://data.humdata.org/dataset/a9455df0-e068-4ef9-8464-90a19586a80d

Fang, J., Xu, C., Wen, Y., Wang, S., Xu, G., Zhao, Y., & Yi, L. (2019). The 2018 Mw 7.5 Palu earthquake: A supershear rupture event constrained by InSAR and broadband regional seismograms. *Remote Sensing*, *11*(11), 1–15. https://doi.org/10.3390/rs11111330

Hanssen, R. F. (2002). *Radar Interferometry Data Interpretation and Error Analysis*. *Remote Sensing and Digital Image Processing* (Vol. 2). United States of America: Kluwer Academic Publishers. https://doi.org/10.1017/CBO9781107415324.004

Ishitsuka, K., Tsuji, T., & Matsuoka, T. (2013). Detection and mapping of soil liquefaction in the 2011 Tohoku earthquake using SAR interferometry. *Earth, Planets and Space*, *64*(12), 1267–1276. https://doi.org/10.5047/eps.2012.11.002

Kobayashi, T., Morishita, Y., & Yarai, H. (2015). Detailed crustal deformation and fault rupture of the 2015 Gorkha earthquake , Nepal , revealed from ScanSAR-based interferograms of ALOS-2. *Earth, Planets and Space*, (2015). https://doi.org/10.1186/s40623-015-0359-z

Natsuaki, R., Nagai, H., Tomii, N., & Tadono, T. (2018). Sensitivity and limitation in damage detection for individual buildings using InSAR coherence-A case study in 2016 Kumamoto earthquakes. *Remote Sensing*, *10*(2). https://doi.org/10.3390/rs10020245

Nielsen, A. a., & Conradsen, K. (1997). Multivariate Alteration Detection (MAD) in Multispectral, Bi-temporal Image Data: A new approach to change detection studies. *Technical Report*, *1*(97), 1–28. https://doi.org/10.1017/CBO9781107415324.004

Plank, S. (2014). Rapid Damage Assessment by Means of Multi-Temporal SAR — A Comprehensive Review and Outlook to Sentinel-1. *Remote Sensing*, *6*(6), 4870–4906. https://doi.org/10.3390/rs6064870

Sandwell, D., Mellors, R., Tong, X., Xu, X., Wei, M., & Wessel, P. (2016). GMTSAR: An InSAR Processing System Based on Generic Mapping Tools (Second Edition), 1–120.

Stramondo, S., Bignami, C., Chini, M., Pierdicca, N., & Tertulliani, A. (2006). Satellite radar and optical remote sensing for earthquake damage detection: results from different case studies. *International Journal of Remote Sensing*, *27*(20), 4433–4447. https://doi.org/10.1080/01431160600675895

Tamkuan, N., & Nagai, M. (2017). Fusion of Multi-Temporal Interferometric Coherence and Optical Image Data for the 2016 Kumamoto Earthquake Damage Assessment. *ISPRS International Journal of Geo-Information*, *6*(7), 188. https://doi.org/10.3390/ijgi6070188

Tamkuan, N., & Nagai, M. (2019). Sentinel-1A Analysis for Damage Assessment: A Case Study of Kumamoto Earthquake in 2016. *MATTER: International Journal of Science and Technology*, *5*(1), 23–35. https://doi.org/10.20319/mijst.2019.51.2335

Yonezawa, C., & Takeuch, S. (1995). Detection of Urban Damage Using Interferometric SAR Decorrelation.

Zebker, H. A., & Villasenor, J. (1992). Decorrelation in interferometric radar echoes. *IEEE Transactions on Geoscience and Remote Sensing*, *30*(5), 950–959. https://doi.org/10.1109/36.175330